Nitrogen assimilation in picocyanobacteria inhabiting the oxygen-deficient waters of the eastern tropical North and South Pacific

Montserrat Aldunate, Carlos Henríquez-Castillo, Qixing Ji, Jessica Lueders-Dumont, Margaret R Mulholland, Bess Ward, Peter von Dassow, Osvaldo Ulloa

LIMNOLOGY
and
OCEANOGRAPHY

ASLO

Limnol. Oceanogr. 00, 2019, 1–17

doi: 10.1002/lno.11315

Nitrogen assimilation in picocyanobacteria inhabiting the oxygen-deficient waters of the eastern tropical North and South Pacific

Montserrat Aldunate,[1,2,3] Carlos Henríquez-Castillo,[1,3] Qixing Ji,[4,a] Jessica Lueders-Dumont,[4] Margaret R. Mulholland,[5] Bess B. Ward,[4] Peter von Dassow,[3,6,7] Osvaldo Ulloa[1,3*]

[1]Departamento de Oceanografía, Universidad de Concepción, Concepción, Chile
[2]Programa de Postgrados en Oceanografía, Universidad de Concepción, Concepción, Chile
[3]Instituto Milenio de Oceanografía, Universidad de Concepción, Concepción, Chile
[4]Department of Geosciences, Princeton University, Princeton, New Jersey, USA
[5]Department of Ocean, Earth and Atmospheric Sciences, Old Dominion University, Norfolk, Virginia, USA
[6]Departmento de Ecología, Pontificia Universidad Católica de Chile, Santiago, Chile
[7]UMI 3614, Evolutionary Biology and Ecology of Algae, Centre National de la Recherche Scientifique-UPMC Sorbonne Universités, PUCCh, UACH, Station Biologique de Roscoff, Roscoff, France

Abstract

Prochlorococcus and *Synechococcus* are the most abundant free-living photosynthetic microorganisms in the ocean. Uncultivated lineages of these picocyanobacteria also thrive in the dimly illuminated upper part of oxygen-deficient zones (ODZs), where an important portion of ocean nitrogen (N) loss takes place via denitrification and anaerobic ammonium oxidation. Recent metagenomic studies revealed that ODZ *Prochlorococcus* have the genetic potential for using different N forms, including nitrate and nitrite, uncommon N sources for *Prochlorococcus*, but common for *Synechococcus*. To determine which N sources ODZ picocyanobacteria are actually using in nature, the cellular ^{15}N natural abundance ($\delta^{15}N$) and assimilation rates of different N compounds were determined using cell sorting by flow cytometry and mass spectrometry. The natural $\delta^{15}N$ of the ODZ *Prochlorococcus* varied from −4.0‰ to 13.0‰ ($n = 9$), with 50% of the values in the range of −2.1–2.6‰. While the highest values suggest nitrate use, most observations indicate the use of nitrite, ammonium, or a mixture of N sources. Meanwhile, incubation experiments revealed potential assimilation rates of ammonium and urea in the same order of magnitude as that expected for total N in several environments including ODZs, whereas rates of nitrite and nitrate assimilation were very low. Our results thus indicate that reduced forms of N and nitrite are the dominant sources for ODZ picocyanobacteria, although nitrate might be important on some occasions. ODZ picocyanobacteria might thus represent potential competitors with anammox bacteria for ammonium and nitrite, with ammonia-oxidizing archaea for ammonium, and with nitrite-oxidizing bacteria for nitrite.

Prochlorococcus and *Synechococcus* are the most abundant free-living photosynthetic microorganisms in the euphotic zone of oligotrophic tropical and subtropical ocean waters (Partensky et al. 1999*a*,*b*). These picocyanobacteria represent ~ 25% of marine primary productivity (Flombaum et al. 2013) and their successful colonization of the global ocean has been attributed to their small size and ability to take up nutrients at high rates (Chisholm 1992), as well as their high within species genetic diversity (Scanlan 2003; Biller et al. 2014).

The structure and pigment content of their photosynthetic apparatus differs between the two picocyanobacteria: *Synechococcus* uses a phycobilisome as the main light-harvesting antenna while *Prochlorococcus* lacks phycobilisomes and uses a complex of chlorophyll-binding proteins (Pcb) (Partensky et al. 1999*b*). The Pcb complex contains divinyl chlorophyll *a* (Chl a_2) and divinyl chlorophyll *b* (Chl b_2). This complex allows them to capture light more efficiently at greater depths (Moore and Chisholm 1999). Indeed, some lineages of *Prochlorococcus* with high ratios of Chl b_2/a_2 content are able to grow at extremely

*Correspondence: oulloa@udec.cl

Additional Supporting Information may be found in the online version of this article.

[a]Present address: Helmholtz Centre for Ocean Research Kiel, Kiel, Germany

low irradiances (< 10 mol quanta m^{-2} s^{-1}), where low Chl b_2/a_2 lineages are incapable of such growth. Conversely, low Chl b_2/a_2 lineages are able to grow maximally at higher light intensities where high Chl b_2/a_2 isolates are inhibited (Moore and Chisholm 1999). Thus, the depth distributions of *Prochlorococcus* lineages are consistent with these characteristics: members of the high light (HL) ecotypes are found mainly in the nutrient-depleted surface waters of the ocean, while members of the low light (LL) ecotypes are dominant at the base of the euphotic zone where nutrients are replete (Goericke et al. 2000; West et al. 2001; Rocap et al. 2003; Johnson et al. 2006; Lavin et al. 2010). While *Prochlorococcus* shows a clear vertical partitioning of ecotypes related principally with light and the availability of nutrients, *Synechococcus* lineages do not show a clear spatial partitioning with depth (Moore et al. 1998; Biller et al. 2014).

As for other phytoplankton, the assimilation of N is central to picocyanobacteria nutrition, with ammonium (NH_4^+) as the preferred N source due to the low energy needed for its assimilation into organic N (Moore et al. 2002). There are indications that *Prochlorococcus* and *Synechococcus* lineages have diverged in the ability to use also other forms of N that are available in the ocean, such as nitrate (NO_3^-) and nitrite (NO_2^-) (Moore et al. 2002; Martiny et al. 2009), cyanate (Fuhrman 2003; Kamennaya and Post 2011), and amino acids (Zubkov et al. 2003). Initially, *Prochlorococcus* was considered unable to use nitrate (NO_3^-), because the original cultured isolates could not use it (Moore et al. 2002). Nevertheless, more recent studies have demonstrated genomic (Martiny et al. 2009; Batmalle et al. 2014; Berube et al. 2015) and indirect physiological (Casey et al. 2007) evidence of NO_3^- assimilation, in both cultured *Prochlorococcus* and natural assemblages of *Prochlorococcus*. Analyzing the genomes of different strains of *Prochlorococcus*, Berube et al. (2015) showed that the genomic configuration of the genes related to the NO_3^- assimilation differed among *Prochlorococcus* strains. They presented evidence of acquisition, loss, and horizontal transfer of NO_3^- assimilation related genes for some HL strains, as well as evidence of retention of those genes in some members of the LL ecotypes during the evolutionary diversification from their common ancestor with *Synechococcus*.

The most basal *Prochlorococcus* lineages found to date are noncultured representatives (LLV and LLVI) inhabiting the secondary chlorophyll maximum (SCM) in the oxygen-deficient waters of the eastern tropical North and South Pacific (ETNP and ETSP), which are characterized as adapted to very low-light and nutrient-rich conditions (Lavin et al. 2010; Ulloa et al. 2012). These SCMs have been found specifically in the oxygen-deficient zones (ODZs), also known as anoxic marine zones (AMZs), that are distinguished from other oxygen minimum zones by the accumulation of nitrite and the complete absence of detectable oxygen using the most sensitive detectors such as the STOX oxygen sensor (detection limits 1–10 nmol L^{-1}; Revsbech et al. 2009; Thamdrup et al. 2012; Ulloa et al. 2012). Nevertheless, these *Prochlorococcus* have recently been shown to drive a cryptic oxygen cycle that possibly fuels aerobic processes such as NO_2^--oxidation (Garcia-Robledo et al. 2017).

In the ODZs, there is an accumulation of NO_2^-, mainly due to dissimilatory nitrate reduction (Ward et al. 2009; Lam and Kuypers 2011) that only takes place when oxygen levels are below 50 nmol L^{-1} (Thamdrup et al. 2012). Within the ODZs, there are high concentrations of inorganic nutrients and a very active nitrogen (N) cycle mediated by anaerobic microorganisms (Lam and Kuypers 2011). The forms and abundance of bioavailable N present, as well as the sources of energy supporting their assimilation, are important factors controlling the growth of *Prochlorococcus* and *Synechococcus*. Any inorganic N taken up must be converted to NH_4^+ for incorporation into vital compounds such as amino acids or nucleic acids (Berges and Mulholland 2008), so assimilation of reduced forms of N such as NH_4^+ or urea is metabolically favored when they are available (García-Fernández et al. 2004; García-Fernández and Diez 2004; Berges and Mulholland 2008). However, the most common forms of N in such extremely ODZs are NO_3^- and NO_2^- (Ulloa et al. 2012) with very low (nmol L^{-1}) to undetectable concentrations of NH_4^+ and undetectable concentrations of urea using standard methods (Thamdrup et al. 2006; Hamersley et al. 2007; Widner et al. 2018*b*). Thus, in contrast to the picocyanobacteria in the primary chlorophyll maximum (PCM) above the oxycline, the ODZ cyanobacteria inhabit a high NO_3^- and NO_2^- environment.

Reconstruction of a metagenome using environmental samples collected from the SCM in the ETSP showed that these ODZ lineages have the genetic potential to assimilate urea and NO_3^- (Astorga-Eló et al. 2015), having a full repertoire of genes involved in NO_3^- transport (*napA*), NO_3^- assimilation (*narB*), and biosynthesis of the Mo-cofactor (*moeA* and *mobA*) necessary for the *narB* function (Flores and Herrero 2005). Astorga-Eló et al. (2015) also suggested that this pathway was retained during *Prochlorococcus* divergence from *Synechococcus* rather than a secondary horizontal gain (Astorga-Eló et al. 2015). This scenario is similar to what occurred in lineage LLIV, a lineage that appears not to be affected by the genome reduction documented in the more recently diverged lineages of *Prochlorococcus* (e.g., HL strain MED4) (Partensky and Garczarek 2010). Lately, Widner et al. (2018*a*) showed that LLIV *Prochlorococcus* inhabiting the ODZ also have genes for the utilization of NH_4^+ and NO_2^-, although no cyanate assimilation related genes were found.

The capacity for utilization of NO_3^- or NO_2^- might confer to ODZ *Prochlorococcus* an ecological advantage over *Prochlorococcus* lineages that do not have the genes needed to assimilate these compounds, allowing them to take advantage of the high NO_3^- concentrations (with respect to NH_4^+ and/or urea) present in the SCM in the ODZs. This capability might also allow ODZ *Prochlorococcus* to avoid competition for NH_4^+ with important groups of microorganisms recycling N in these regions, such as anammox bacterial and ammonia-oxidizing archaea. Thus,

a further knowledge about the metabolic capabilities and physiology of ODZ *Prochlorococcus* and the less abundant, but present, *Synechococcus*-like lineages inhabiting the SCM within the ODZ is essential for understanding their role in ODZs and how they may use this niche as an advantage over other lineages that cannot consume NO_3^-. Therefore, in this work, we focus on testing the hypothesis, based on apparent genomic potential, that *Prochlorococcus* uses NO_3^- as a N source for its assimilative metabolism.

Stable isotopes analysis is a powerful tool for investigating this hypothesis. $\delta^{15}N$ notation represents the deviation between the ratio of the two stable isotopes of N ($^{15}N/^{14}N$) contained in the samples (particulate organic nitrogen and/or selected sorted picoplanktonic groups) compared with the ratio of these same two stable isotopes of N contained in the atmospheric N_2 (standard) (Owens 1987). Comparing the $\delta^{15}N$ of the organisms that inhabit an environment with the $\delta^{15}N$ of the different N sources available for assimilation in a specific environment (e.g., $\delta^{15}N$ of NO_3^- and NO_2^-) can help determine which sources of N are being used by the organisms. Previous work has coupled the use of stable isotopes and cell sorting, allowing the characterization of the N content and the natural abundance $\delta^{15}N$ signature of distinct components of the particulate nitrogen suspended in Sargasso Sea surface waters (Fawcett et al. 2011) and specific uptake rates of different $\delta^{15}N$-labeled sources of N by *Prochlorococcus* (Casey et al. 2007). In this study, we analyzed the natural abundance of $\delta^{15}N$ of suspended particulate organic nitrogen (PON_{sus}) and *Prochlorococcus* and *Synechococcus*-like cells sorted from the microbial community inhabiting the SCM (and PCM when SCM was present) at several stations in the ODZ in both ETNP and ETSP. These $\delta^{15}N$ data were compared with literature values of $\delta^{15}N$ natural abundance signatures of different sources of N. Complementary experimental evidence for the uptake of N compounds was derived from onboard tracer incubations in which natural seawater samples collected from the SCM were amended with ^{15}N-labeled NO_3^-, NO_2^-, NH_4^+, and urea to measure potential assimilation rates in flow cytometrically sorted groups of picoplankton.

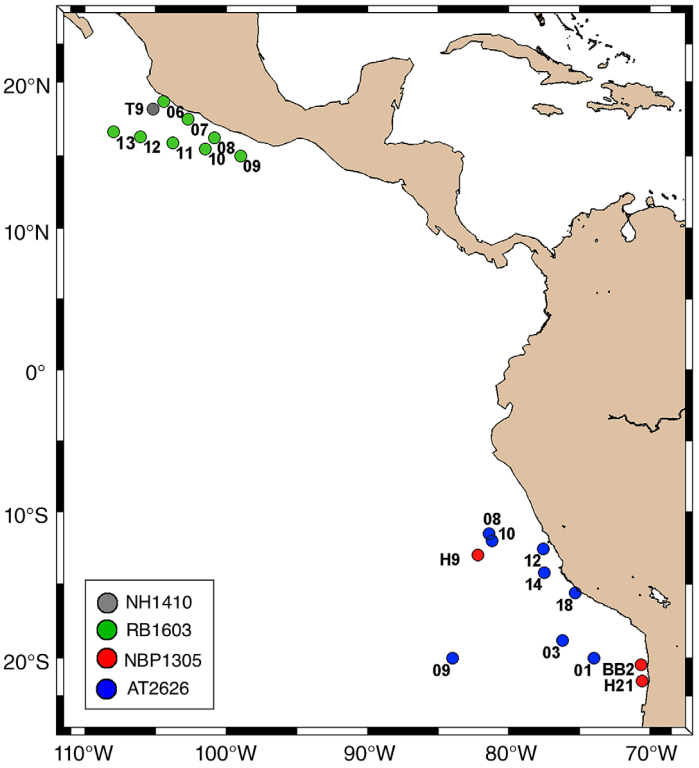

Fig. 1. Map with the sampled stations in the ETNP (cruises: NH14010 and RB1603) and the ETSP (cruises: NBP1305 and AT2626). [Color figure can be viewed at wileyonlinelibrary.com]

Materials and methods

Sampling site and field collection

Samples were obtained from the ODZs of the ETNP and ETSP, during four cruises: NH1410 (May 2014) and RB1603 (April 2016) for the ETNP, and NBP1305 (June 2013) and AT2626 (January 2015) for the ETSP (see station map in Fig. 1). Samples were taken from two depths, one from the PCM and the other from the SCM. The collection of water samples at both depths was performed using a pump profiler system (PPS); an instrument that pumps water directly from the desired depth while profiling the water column with an attached conductivity-temperature-depth (CTD) system (Seabird SBE-19 plus for ETNP and Seabird SBE-25 for ETSP), which provides continuous determinations of salinity, temperature, depth, as well as dissolved oxygen (Seabird SBE 43 oxygen sensor; all cruises) and in vivo fluorescence (WETStar for ETNP cruise and ECO-AFL/FL for ETSP cruises, both WET Labs fluorometers).

NO_3^-, NO_2^-, and urea samples were run on an Astoria Pacific autoanalyzer using standard colorimetric methods according to the manufacturers specifications. NH_4^+ was determined using the fluorometric method of Holmes et al. (1999). In April 2016 (ETNP; cruise RB1603), seawater was pumped into the laboratory and connected to an auto analyzer for nutrients continuous profiles for NO_3^-, NO_2^-, and NH_4^+, binned to one measurement per second.

$\delta^{15}N$ natural abundance

PON_{sus} (0.3–3 μm size fraction) $\delta^{15}N$ natural abundance was determined by filtering 2–3 L of seawater though a 3-μm pore size polycarbonate membrane filter and collecting the microbial biomass on a precombusted (500°C for 6 h) 0.3-μm glass fiber filter (Sterlitech GF-75; 0.3 μm nominal pore size). The GF-75 filters were dried onboard or frozen in liquid nitrogen. Once in the laboratory, GF-75 filters were fumed with HCl vapors for 8 h to drive off inorganic C and then dried and encapsulated in tin capsules for analysis at the University of California Davis Stable Isotope Facility (mass detection limit 20 μg of N).

For determining $\delta^{15}N$ natural abundance of sorted groups of cells, 4 L of seawater from the PCM and SCM depths were collected in plastic carboys protected from sunlight. This water was immediately filtered at a very low speed using a peristaltic pump in order to concentrate the cells of this community on 0.4 μm pore size polycarbonate filters after a 3-μm pore size polycarbonate prefilter. To fix the cells, the filters were placed in 4-mL cryovials with 200 μL of 10% formaldehyde solution and filled to 4 mL using 0.22-μm prefiltered seawater (0.5% formaldehyde final concentration). After 1 h of incubation in the dark at 4°C, the samples were gently agitated and stored in liquid nitrogen until reaching land, upon which the samples were stored at −80°C until processing.

Incubation experiments

For incubation experiments, water was collected in a 20-liter glass bottle and purged for 20 min with a mixture of 800 ppm CO_2 balanced He in order to avoid any oxygen contamination during the sampling. This water was siphoned to 6–12 custom-made incubation bottles (1.1 liter) for anoxic experiments. These bottles were previously purged with the same mixture of He/CO_2 and were filled overflowing the water approximately 1.5 times their volume. Finally, the bottles were placed in an incubator inside a temperature-controlled cold van (see diagram in Supporting Information Fig. S1). The incubator was composed of a temperature-controlled water bath, two blue LED panels with controlled intensities of light, as well as of magnetic stirrers that prevent stratification of the water inside each incubation bottle. The incubation conditions were set to simulate in situ temperature (ranging between 14°C and 16°C depending on the station) and light intensities (10–30 μmol photons m^{-2} s^{-1}). Four different ^{15}N-labeled compounds (Cambridge Isotope Laboratories) were used to assess the potential N assimilation rates in the picoplanktonic community. Because environmental nutrient concentrations were measured only after incubations were started, the enrichment of the N sources exceeded 10–15% -the enrichment recommended for in situ assimilation rates- and so represents potential assimilation rates (Dugdale and Wilkerson 1986). Measured final concentrations of ^{15}N-NO_3^- and ^{15}N-NO_2^- were 5.5 μmol L^{-1} and 0.2 μmol L^{-1}, respectively. These concentrations represented enrichments of 19.6–27.2% for ^{15}N-NO_3^- and 47.6% for ^{15}N-NO_2^-. The in situ concentrations of urea were undetectable (detection limit 70 nmol L^{-1}) and in the nmol L^{-1} ranges for NH_4^+ (detection limit 10 nmol L^{-1}). The additions of ^{15}N-Urea and ^{15}N-NH_4^+ were 0.2 μmol L^{-1} and 0.18 μmol L^{-1} final concentration, respectively, representing an enrichment of 74.1% for ^{15}N-urea and 88.2% for ^{15}N-NH_4^+. Since urea was undetectable, the detection limit of the method (70 nmol L^{-1}) was used for the enrichment calculation. After 12 h of incubation, the picoplankton from each bottle was concentrated by filtration and stored as described above for ^{15}N natural abundance measurements.

Flow cytometric cell sorting

Both the natural abundance and isotopically enriched samples were analyzed following Fawcett et al. (2011) with some modifications: samples were thawed to room temperature and were gently stirred to detach the cells from the filter. When necessary, samples were diluted using 0.22 μm filtered NaCl (3.5% by weight). Isolation of groups was performed using an InFlux® Flow Cytometer-Cell Sorter (formerly Cytopeia, BD Biosciences, San Jose, CA, U.S.A.) equipped with five lasers (488-nm [200 mW], 457-nm [300 mW], 532-nm [150 mW], 355-nm [100 mW], and 640-nm [50 mW]) using an 86-μm ceramic black nozzle tip and a sheath pressure of 227.5 kPa. Sheath fluid was prepared daily using molecular biology grade NaCl (3.5% by weight) and purified (Milli-Q) water, filtered through 0.22-μm Steripak filter unit (Merck Millipore, SPGPM20RJ) and passed through an in-line 0.22-μm Sterivex filter unit (Merck Millipore, SVGVL10RC). Ultra rainbow fluorescent particles (1 and 3 μm, Spherotech, Lake Forest, IL, U.S.A.) were used for alignment and calibration. For picophytoplanktonic cells, sort gates were optimized based on the autofluorescence of each group. *Prochlorococcus* cells were gated based on their red fluorescence (692/40 nm; for each fluorescence emission filter, the center wavelength and band-pass width are given) using a combination of the 457 and 488 nm blue lasers. *Synechococcus*-like cells were gated based on their orange fluorescence (530/40 nm) using the 488 (blue) and 532 nm (green) lasers and photosynthetic picophytoeukaryotes (PPEs) were gated based on their red fluorescence (692/40 nm) using the 488 nm blue laser. Events were triggered on the forward light scatter. Nonpigmented cells were stained with Sybr Green I as described in Marie et al. (1999). Events were triggered based on green (530/15) fluorescence excited by the 488 nm laser and cells detected by their green fluorescence (530/15 nm) and absence of red fluorescence. Samples were run at an average flow rate of 30 μL min^{-1}, monitored with a liquid flowmeter (Sensirion, U.S.A.) and the event rate was 10,000–15,000 events s^{-1}. Cells were sorted in purity mode using two tubes configuration, the drop delay was calculated using the calibration procedure with the Spigot Software and an epifluorescence microscope. Cytometry files were analyzed with the FlowJo Software (FlowJo, Ashland, OR, U.S.A.) and plotted using R software (ggplot package). The groups isolated were filtered on 0.3 μm pore size precombusted glass fiber filters (Sterlitech GF-75; 0.3 μm nominal pore size) and dried in an oven at 40°C. These filters were placed in precombusted aluminum envelopes and stored free of humidity until persulfate oxidation.

Persulfate oxidation and denitrifier method

The filters containing both natural abundance and ^{15}N-enriched cells were placed in 4-mL precombusted (500°C for 5 h) glass vials. Two milliliters of persulfate-oxidation reagent (POR; 3 g of NaOH in 60 mL of deionized water + 3 g of 5X recrystallized persulfate in 60 mL of deionized water) was added to each vial. Isotopic reference for organic-bound

nitrogen (USGS40, USGS41, L-glutamic acid) and blanks filters were treated with the same 2 mL of POR. All samples, standards, and blanks were autoclaved at 121°C for 30 min. At this point, all the organic nitrogen content was oxidized to NO_3^- and its concentration was measured by reduction to nitric oxide and detection in a chemiluminescent detector (Teledyne model #200 EU; Garside 1982). To obtain $\delta^{15}N$ values, we used the "denitrifier method" (Sigman et al. 2001; 10–20 nmol N optimal), which is based on the isotopic analysis of nitrous oxide (N_2O) generated by the action of denitrifying bacteria that convert NO_3^- to N_2O and lack N_2O-reductase. The isotopic composition of the N_2O was measured by gas chromatography-isotope ratio mass spectrometry using a modified ThermoFinnigan GasBench II and Delta V. Final measurements were corrected by blanks.

N assimilation rates calculations

The cell-specific uptake rates (ρDINcells; fg N cell^{-1} h^{-1}) of dissolved inorganic nitrogen (DIN) were calculated for each N source. The equations used are provided in Dugdale and Wilkerson (1986) with some modification applied to cell-specific assimilation rates:

$$V = \frac{R_{(\text{cells})}}{R_{(\text{DIN})}} \times T \quad (1)$$

$$\rho\text{DINcells} = V \times \frac{N}{\text{CS}} \quad (2)$$

where V is the specific uptake rate (h^{-1}); $R_{(\text{cells})}$ = ^{15}N atom percent in the cells at the end of the incubation – ^{15}N atom percent in the cells initial; $R_{(\text{DIN})}$ = ^{15}N atom percent enrichment in DIN – ^{15}N atom percent in the cells initial; T represents the incubation time (hours); N represents the amount of N in the analyzed sorted cells (fg N); and CS = number of sorted cells for isotope analysis (cells).

Group-specific uptake rates (ρDIN group; nmol L^{-1} d^{-1}) were calculated as follows:

$$\rho\text{DINgroup} = \rho\text{DINcells} \times \text{ISA} \quad (3)$$

where ISA is the average in situ abundance of each group of sorted cells (cells L^{-1}).

When the tracer additions resulted in initial enrichments exceeding 50%, rates should be considered as potential uptake.

The detection limit of each uptake rate was calculated in order to determine if those rates were significantly different from zero. The detection limit was calculated following the specifications of Santoro et al. (2013) as the N (NH_4^+, urea, NO_3^-, NO_2^-) uptake rate necessary to cause a 1‰ increase in $\delta^{15}N$ of sorted cells from the initial value ($\delta^{15}N$ natural abundance). The 1‰ value represents twice the precision of $\delta^{15}N$ analysis using the denitrifier method (precision = 0.5‰; Sigman et al. 2001; McIlvin and Casciotti 2011).

Statistical analysis

Statistical differences among natural $\delta^{15}N$ for PON_{sus} and sorted groups of cells (*Pro*, *Syn*) were tested using Wilcoxon and the Kruskal-Wallis test. Statistical significance was set at the 0.05 level. The correlations between $\delta^{15}N$ of *Prochlorococcus*, $\delta^{15}N$ *Synechococcus*-like, and environmental factors (nutrient concentrations and light %) were calculated using Pearson's correlation analysis. The variables were logarithmic transformed as $\text{Log}_{10}(X + 1)$ and the Pearson's correlation coefficients were tested for significance at $\alpha = 0.05$ using XLStat software (AddinSoft SARL).

Results

Water column structure and nutrient content

The structure of the water column at all experimental stations exhibited a SCM in the ODZ like the examples represented in Fig. 2 (summarized in Tables 1–2). The O_2 profile shows the typical distribution with a surface oxygenated layer ranging in depth between 22 and 80 m for the ETNP, and 34 and 89 m for the ETSP, with O_2 concentrations ranging from 197 to 215 μmol L^{-1} for the ETNP and 208 to 267 μmol L^{-1} for the ETSP. Below the mixed layer, O_2 concentrations decreased rapidly depth, reaching anoxia at 62–130 m depth (depending of the station and proximity to the coast). The SCM was found within the upper anoxic layer, with the peak at average depths of 114 m (SD = 28 m; min = 90 m; max = 160 m) for the ETNP and 100 m (SD = 21 m; min = 68 m; max = 130 m) for the ETSP. The SCM varied in intensity (see examples in Fig. 2A,D) with a maximum fluorescence equaling or almost doubling that of the PCM at some stations (Table 1).

NH_4^+ concentrations (detection limit = 10 nmol L^{-1}) for the SCM presented no major differences between the two regions, reaching an average of 18.4 nmol L^{-1} for the ETNP (SD = 28.3 nmol L^{-1}; min = bdl; max = 72.4 nmol L^{-1}) and 27.5 nmol L^{-1} for the ETSP (SD = 29.2 nmol L^{-1}; min = bdl; max = 88.4 nmol L^{-1}). NH_4^+ concentrations in the PCM tended to be higher, reaching on average 36.2 nmol L^{-1} (SD = 62.3 nmol L^{-1}, min = bdl, max = 191.9 nmol L^{-1}) in the ETNP and one order of magnitude more abundant in the ETSP with 481.2 nmol L^{-1} (SD = 211.2 nmol L^{-1}; min = 108.2 nmol L^{-1}; max = 822.7 nmol L^{-1}) (Table 2). Samples for urea determination were obtained from both oceans in two cruises (ETNP-RB1603 and ETSP-AT2626), but almost all measurements for the SCM were below the detection limit of the method (70 nmol L^{-1}) with only two stations of the cruise RB1603 reaching concentrations of 0.22 μmol L^{-1} (Sta. 9) and 1.02 μmol L^{-1} (Sta. 10). NO_3^- and NO_2^- profiles (Fig. 2B,E) showed the typical structure for an ODZ (Ulloa et al. 2012). In the surface, both nutrients were depleted, with an accumulation for NO_3^- below the oxycline and of NO_2^- in anoxic waters. In the ETNP (Fig. 2, upper panels), the NO_2^- accumulation (and secondary drop in NO_3^-) was below the *Prochlorococcus* SCM, while in the ETSP (Fig. 2, lower panels), the SCM was small and NO_2^- accumulated (and NO_3^- decreased) within the

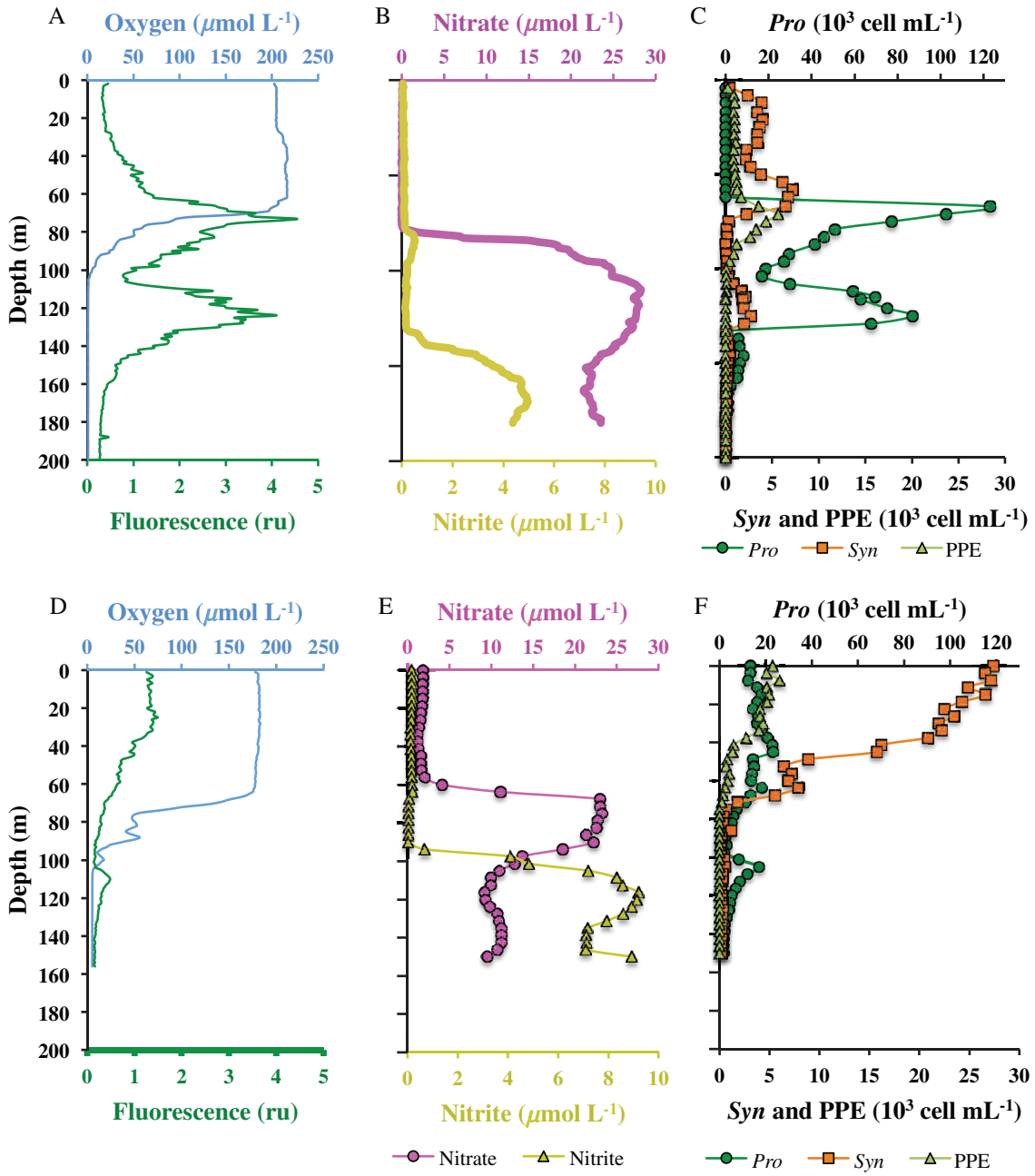

Fig. 2. Examples of environmental conditions of microbial communities inhabiting the SCM in the ODZs from the ETNP (top panels) and ETSP (bottom panels). Panels (**A**) and (**D**) show oxygen and fluorescence (in relative units, ru) profiles (CTD + fluorometer). Panels (**B**) and (**E**) show nitrate and nitrite profiles measured in continuous flow coupling the PPS and an autoanalyzer (**B**) and a high-resolution sampling (**E**). Panels (**C**) and (**F**) show cell count ($\times 10^3$ cell mL^{-1}) profiles of picophytoplankton components obtained by a high-resolution sampling analyzed by flow cytometry. Dark green circles indicate *Prochlorococcus*, light green triangles indicate PPE, and orange squares represent *Synechococcus*-like. [Color figure can be viewed at wileyonlinelibrary.com]

SCM. Nutrient concentrations within the PCM and SCM for all station sampled are shown in Table 2.

Flow cytometric analysis of picoplankton composition

Flow cytometric analysis showed that the picophytoplanktonic communities in anoxic subsurface waters differed consistently from those in oxic surface waters in both abundance and composition (see examples in Fig. 2C,F): picocyanobacteria were numerically dominant in the PCM, while PPEs were also present with abundances ranging between 800 and 96,000 cells mL^{-1} (Supporting Information Table S1). In contrast, SCM communities were mainly composed of *Prochlorococcus* cells and to a lesser extent of *Synechococcus*-like cells (yellow/orange fluorescent), with almost no detectable PPE

Table 1. Flow cytometric analysis of the microbial community at the peak depth of the SCM for the ETNP and ETSP, including: cruise name; station; position (latitude and longitude); peak depth of the SCM reported in meters; the percent of incident light at the SCM peak depth (light%); *Prochlorococcus* (*Pro*), *Synechococcus*-like (*Syn*), PPE, fluorescent picoplankton (Fluor. Picoplank. = *Pro* + *Syn* + PPE), NFP, total picoplanktonic community (Total Picoplank. = *Pro* + *Syn* + PPE + NFP) abundances (10^3 cells mL^{-1}); *Prochlorococcus* relative abundance (in %) to the fluorescent picoplankton and to the total picoplankton; fluorescence of SCM relative to PCM. ND indicates none were detected.

Cruise	Station	Lat. (N)	Long. (W)	Peak depth (m)	Light (%)	*Pro* (× 10^3 cells mL^{-1})	*Syn* (× 10^3 cells mL^{-1})	PPE (× 10^3 cells mL^{-1})	Fluor. Picoplank. (×10^3 cells mL^{-1})	NFP (× 10^3 cells mL^{-1})	Total picoplankton (×10^3 cells mL^{-1})	*Pro* Rel. Ab. to Fluor. Picoplank. (%)	*Pro* Rel. Ab. to Total Picoplank. (%)	Fluor. of SCM relative to PCM
ETNP														
NH1410	T9	18.200	105.199	90	1.39	70	7.4	0.09	77.5	476	553	90	12.7	1.30
RB1603	6	18.688	104.417	90	0.01	53	1.3	0.00	54.3	372	426	98	12.4	0.57
RB1603	7	17.500	102.700	93	0.02	78	2.0	0.00	80.0	664	744	98	10.5	0.71
RB1603	8	16.251	100.843	97	ND	58	1.8	0.00	59.8	586	646	97	9.0	0.06
RB1603	9	15.000	99.000	98	ND	40	0.9	0.00	40.9	511	552	98	7.2	0.21
RB1603	10	15.471	101.503	128	ND	13	0.5	0.00	13.5	671	684	96	1.9	0.36
RB1603	11	15.903	103.800	115	ND	70	2.1	0.00	72.1	421	493	97	14.2	0.90
RB1603	12	16.316	106.092	156	ND	22	0.2	0.00	22.2	402	424	99	5.2	0.45
RB1603	13	16.778	108.397	160	ND	7	0.2	0.00	7.2	398	405	97	1.7	0.17
Min	—	—	—	**90**	—	**7**	**0.2**	**0.00**	**7.2**	**372**	**405**	**90**	**1.7**	**0.06**
Max	—	—	—	**160**	—	**78**	**7.4**	**0.09**	**80.0**	**671**	**744**	**99**	**14.2**	**1.30**
Average	—	—	—	**114**	—	**46**	**1.8**	**0.01**	**47.5**	**500**	**548**	**97**	**8.3**	**0.52**
SD	—	—	—	**28**	—	**26**	**2.2**	**0.03**	**27.9**	**116**	**123**	**2**	**4.6**	**0.40**
ETSP														
NBP1305	H9	13.002	82.199	110	0.35	17	0.5	0.00	17.5	673	691	97	2.5	0.33
NBP1305	H21	21.500	70.582	79	0.69	7	0.7	0.00	7.7	436	444	91	1.6	0.33
NBP1305	BB2	20.526	70.712	80	0.31	13	1.8	0.04	14.8	896	911	88	1.4	0.18
AT2626	1	20.002	74.005	105	0.01	15	2.0	0.00	17.0	217	234	88	6.4	0.31
AT2626	3	18.798	76.200	98	0.01	144	37.6	3.98	185.6	5220	5406	78	2.7	1.91
AT2626	8	11.502	81.411	112	0.01	98	1	0.00	99.0	661	760	99	12.9	0.62
AT2626	9	11.999	84.001	130	ND	24	2	0.00	26.0	329	355	92	6.8	0.36
AT2626	10	11.998	81.198	110	0.07	46	1	0.82	47.8	196	244	96	18.9	1.12
AT2626	12	12.545	77.593	127	ND	28	0.2	0.00	28.2	497	525	99	5.3	0.15
AT2626	14	14.198	77.499	78	ND	18	1.1	0.00	19.1	492	511	94	3.5	0.02
AT2626	18	15.591	75.335	68	0.05	20	1.0	0.00	21.0	878	899	95	2.2	0.39
Min	—	—	—	**68**	—	**7**	**0.2**	**0.00**	**7.7**	**196**	**234**	**78**	**1.4**	**0.02**
Max	—	—	—	**130**	—	**144**	**37.6**	**3.98**	**185.6**	**5220**	**5406**	**99**	**18.9**	**1.91**
Average	—	—	—	**100**	—	**39**	**4.4**	**0.44**	**44.0**	**954**	**998**	**93**	**5.8**	**0.52**
SD	—	—	—	**21**	—	**43**	**11.0**	**1.20**	**53.3**	**1434**	**1481**	**6**	**5.5**	**0.54**

Table 2. Nutrient analysis at the peak depth of the PCM and SCM for stations sampled in the ETNP and ETSP. Cruise name, station, peak depth, and NH_4^+, urea, NO_3^- and NO_2^- concentrations. NA indicates no available data and bdl is below detection limit.

		PCM					SCM				
Cruise	**Station**	**Peak depth (m)**	NH_4^+ (nmol L^{-1})	**Urea** (μmol L^{-1})	NO_3^- (μmol L^{-1})	NO_2^- (μmol L^{-1})	**Peak depth (m)**	NH_4^+ (nmol L^{-1})	**Urea** (μmol L^{-1})	NO_3^- (μmol L^{-1})	NO_2^- (μmol L^{-1})
ETNP											
NH1410	T9	40	191.9	NA	NA	NA	90	63.0	NA	NA	NA
RB1603	6	30	14.6	NA	0.1	0.0	90	bdl	NA	28.2	0.0
RB1603	7	49	25.7	bdl	5.4	0.8	93	bdl	bdl	26.5	0.4
RB1603	8	35	bdl	bdl	0.1	0.2	97	bdl	NA	29.4	0.2
RB1603	9	45	70.7	0.01	0.0	0.5	98	72.4	0.22	27.6	1.0
RB1603	10	76	9.4	0.10	0.1	0.0	128	11.0	1.02	26.8	0.2
RB1603	11	78	bdl	bdl	0.1	0.1	115	bdl	bdl	24.9	0.2
RB1603	12	95	bdl	0.07	0.0	0.1	156	bdl	bdl	26.8	0.2
RB1603	13	69	bdl	bdl	0.1	0.1	160	bdl	bdl	26.2	0.1
Min		30	bdl	bdl	0.0	0.0	90	bdl	bdl	24.9	0.0
Max		95	191.9	0.10	5.4	0.8	160	72.4	1.02	29.4	1.0
Average		**57**	**36.2**	**0.06**	**0.7**	**0.2**	**114**	**18.4**	**0.62**	**27.0**	**0.3**
SD		**23**	**62.3**	**0.05**	**1.9**	**0.3**	**28**	**28.3**	**0.57**	**1.3**	**0.3**
ETSP											
NBP1305	H9	25	225.5	NA	1.5	0.1	110	bdl	NA	9.9	8.3
NBP1305	H21	23	504.4	NA	2.9	0.1	79	88.4	NA	8.2	5.1
NBP1305	BB2	24	570.0	NA	3.9	0.2	80	63.0	NA	10.9	3.9
AT2626	1	41	108.2	NA	NA	1.0	105	56.7	NA	NA	0.4
AT2626	3	35	513.2	bdl	NA	0.3	98	22.8	bdl	14.6	0.1
AT2626	8	40	668.7	bdl	8.8	2.0	112	bdl	bdl	24.2	0.5
AT2626	9	34	598.7	bdl	5.5	0.5	130	bdl	bdl	29.3	0.2
AT2626	10	50	237.9	bdl	15.4	0.3	110	bdl	bdl	17.8	5.2
AT2626	12	25	567.7	bdl	4.6	0.1	127	11.1	bdl	25.6	1.5
AT2626	14	20	476.3	bdl	1.0	0.2	78	22.2	bdl	20.6	1.2
AT2626	18	29	822.7	bdl	7.1	1.6	68	24.1	bdl	5.0	11.4
Min		20	108.2	bdl	1.0	0.1	68	bdl	bdl	5.0	0.1
Max		50	822.7	bdl	15.4	2.0	130	88.4	bdl	29.3	11.4
Average		**31**	**481.2**	**bdl**	**5.6**	**0.6**	**100**	**27.5**	**bdl**	**16.6**	**3.4**
SD		**9**	**211.2**	**bdl**	**4.4**	**0.7**	**21**	**29.2**	**bdl**	**8.2**	**3.8**

(Table 1; Supporting Information Fig. S2). The abundance of *Prochlorococcus* at the peak of the SCM varied among stations (Table 1). On average, the abundance of *Prochlorococcus* was 46×10^3 cells mL^{-1} (SD = 26×10^3 cells mL^{-1}) for the ETNP and 39×10^3 cells mL^{-1} (SD = 43×10^3 cells mL^{-1}) for the ETSP, representing 8.3% and 5.8% of the total picoplanktonic community respectively. Moreover, *Prochlorococcus* represented 97% and 93% of the total fluorescent picoplankton for the ETNP and ETSP, respectively (Table 1). Despite this variability, *Prochlorococcus* were always one order of magnitude more abundant than *Synechococcus*-like within the SCM. The remaining 91.7–94.2% of the picoplankton community is referred to as nonfluorescent picoplankton (NFP) and is composed of heterotrophic or chemoautotrophic bacteria and archaea.

$\delta^{15}N$ of PON_{sus} and sorted components of the PCM and SCM picoplanktonic community

The natural abundance $\delta^{15}N$-PON_{sus} in both the PCM and SCM showed a high variability ranging from 5.8‰ to 18.9‰ in the PCM and from 4.3‰ to 16.6‰ in the SCM (Fig. 3). These $\delta^{15}N$ values were always positive, and, in the case of the SCM, far from the $\delta^{15}N$ previously measured for NO_2^- (negative) (Table 3), but in some cases as high as those reported for NO_3^- (Table 3; Peters et al. 2018).

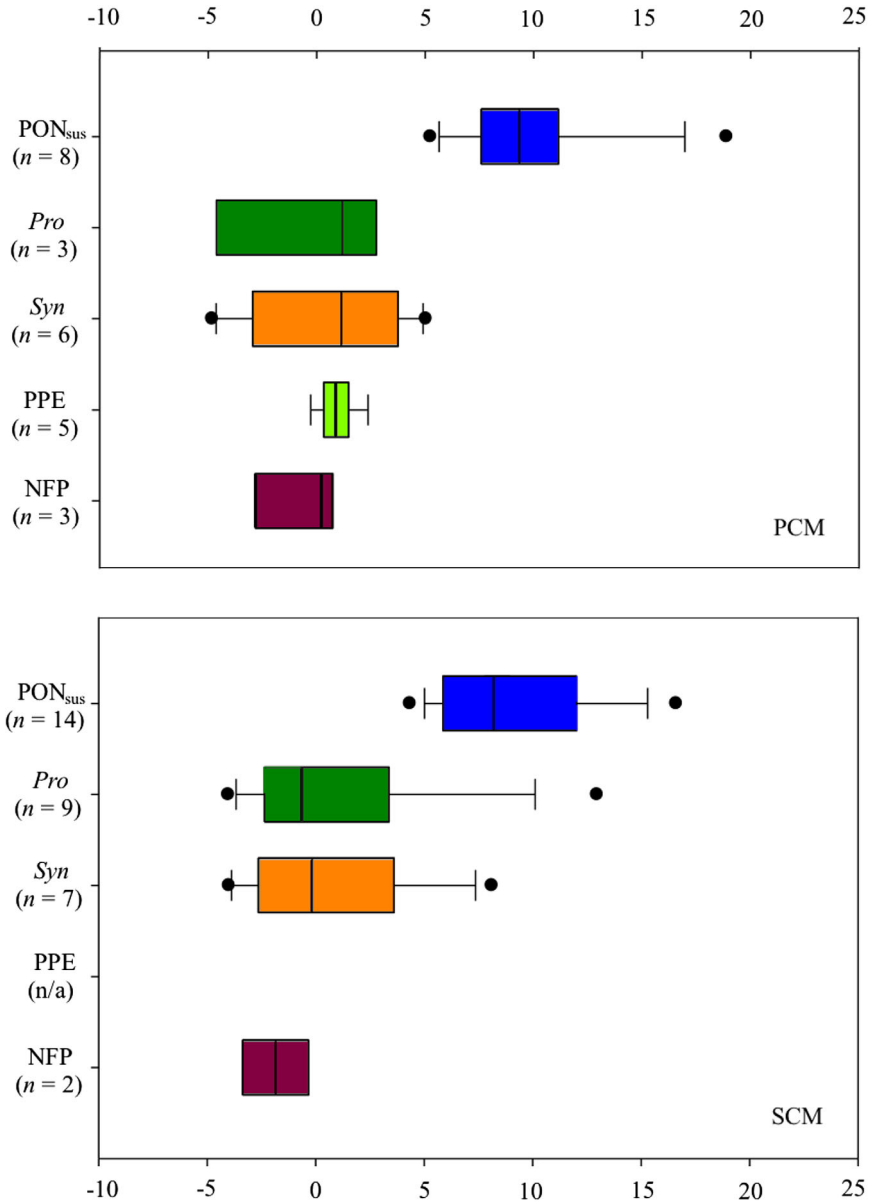

Fig. 3. Boxplot of the $\delta^{15}N$ natural abundance from PON_{sus} (0.3–3.0 μm size fraction) and the $\delta^{15}N$ of sorted picoplankton components from the PCM (top panel) and SCM (bottom panel): *Prochlorococcus* (*Pro*) and *Synechococcus*-like (*Syn*), PPE, and NFP. *n* is the number of measurements per group and n/a indicates that data were not available. [Color figure can be viewed at wileyonlinelibrary.com]

Table 3. $\delta^{15}N$ (‰) for different dissolved N sources in the ODZs and kinetic isotope effect ε (‰) during the assimilation of these sources.

N source	$\delta^{15}N$ (‰)	Study area	Reference	ε_{assim} (‰)	Reference
Nitrate	12.4 ± 0.6 and 17.2 ± 0.6 (ETNP)	TOP ODZ	Casciotti and McIlvin (2007) (ETNP)	2–5	Granger et al. (2010)
	8.2–30.1 (ETSP)		K. Casciotti pers. comm. (ETSP)		
Nitrite	−16.0 ± 2.6 and −17.8 ± 0.9	TOP ODZ ETNP	Casciotti and McIlvin (2007)	1	Sigman and Casciotti (2001)
Ammonium*	Estimated by ~7.1 ± 4.2 (PON_{sus})	TOP ODZ ETNP/ETSP	This study	20	Waser et al. (1998)
	Estimated by ~5.1 (PON_{sk})		Fuchsman et al. (2018) (ETNP)		
Urea*	Estimated by ~7.1 ± 4.2 (PON_{sus})	TOP ODZ ETNP/ETSP	This study	0–0.7	Waser et al. (1998)
	Estimated by ~5.1 (PON_{sk})		Fuchsman et al. (2018) (ETNP)		

*No measurements are available in literature. The estimations are on base of the average obtained by suspended PON in the SCM (PON_{sus} ~ 10‰) and sinking PON (PON_{sk} ~ 8.1‰) minus ε < 3‰ estimated for degradation (Sigman and Casciotti 2001) More details are available in Supporting Information Table S1.

Using a flow cytometer cell sorter, we were able to identify and sort different groups comprising the picophytoplanktonic community inhabiting the SCM. Once the groups were identified, we sorted them and analyzed them to obtain the natural abundance $\delta^{15}N$ for each group (Fig. 3; see summary of the oceans, cruises, stations, and chlorophyll peaks of the samples considered in this study and the isotopic analyses available in each one in Supporting Information Table S2). The values of $\delta^{15}N$ for sorted *Prochlorococcus* and *Synechococcus*-like also showed a high variability among different stations in both the PCM and SCM (Fig. 3 and Supporting Information Table S2). *Prochlorococcus* variability in the SCM was 23% higher than the variability shown by PON_{sus} (the total seston community from which *Prochlorococcus* was sorted) whereas *Synechococcus*-like variability was 8% lower. The $\delta^{15}N$ for *Prochlorococcus* inhabiting the SCM ranged from −4.0‰ to 13.0‰ (Fig. 3). However, the distribution of the data shows that 50% of the values (n = 9) ranged from −2.1‰ to 2.6‰, with a median of −0.6‰ and an average of 1.2‰. In the case of *Synechococcus*-like, $\delta^{15}N$ values presented a similar distribution to *Prochlorococcus*, with total values ranging from −4.0‰ to 8.1‰ and 50% of the data (n = 7) were distributed between −1.9‰ and 2.9‰, with a median of −0.2‰ and an average of 0.9‰. Despite the similar distribution, the highest value of $\delta^{15}N$ for *Synechococcus*-like was not as high as the highest $\delta^{15}N$ value for *Prochlorococcus* (Fig. 3). The multiple-pairwise comparisons among $\delta^{15}N$-PON_{sus}, $\delta^{15}N$-*Pro*, and $\delta^{15}N$-*Syn* for the SCM indicate that there are significant differences between $\delta^{15}N$-PON_{sus} vs. $\delta^{15}N$-*Pro* and $\delta^{15}N$-PON_{sus} vs. $\delta^{15}N$-*Syn* at a 95% confidence level. However, no significant differences were found between $\delta^{15}N$-*Pro* vs. $\delta^{15}N$-*Syn* (Supporting Information Table S3). Only three measurements of $\delta^{15}N$ were available for *Prochlorococcus* inhabiting the PCM, and these measurements present no significant differences with the measurements available for *Prochlorococcus* inhabiting the SCM (Supporting Information Table S4). PPEs were only found in the PCM and exhibited $\delta^{15}N$ values ranging from −0.3‰ to 2.4‰, while 50% of the data (n = 5) ranged from 0.5‰ to 1.2‰. Few measurements for $\delta^{15}N$-NFP were obtained from the PCM and SCM, with average values of −0.9 (n = 3) and −1.8 (n = 2), respectively. The NFP was not included in the statistical analysis due to the low number of measurements available for this group.

Nitrogen assimilation rates

All N uptake rates were above the detection limit (for detection limit results, see Supporting Information Table S5). In the case of the oxidized N forms (Fig. 4A; Table 4), *Prochlorococcus* showed the lowest cell-specific uptake rates of oxidized N forms while NFP showed a preference for NO_3^-, assimilating up to 7.1 times more NO_3^- than NO_2^-. This rate was approximately 7.6 times higher than the NO_3^- uptake rates calculated for *Prochlorococcus* and almost 4.3 times higher than rates calculated for *Synechococcus*-like. *Prochlorococcus* showed very low uptake rates for both NO_2^- and NO_3^-. In contrast, while NO_3^- uptake rates by *Synechococcus*-like were low, NO_2^- uptake rates were 11.4 and 12.5 times higher than those observed for *Prochlorococcus* and NFP, respectively.

The potential cell-specific uptake rates of reduced N forms (Fig. 4B; Table 4) show that NFP and *Prochlorococcus* have higher uptake rates for NH_4^+ compared with urea. In the case of NFP, uptake of NH_4^+ exceeded uptake of urea by 2.0-fold, while in *Prochlorococcus* NH_4^+ uptake exceeded urea uptake by only 1.2-fold. *Synechococcus*-like showed a strong preference for urea uptake and rates were 5.2 times the urea uptake rates measured for NFP and 4.1 times those of *Prochlorococcus*.

We also estimated the group-specific uptake rates (ng N L^{-1} d^{-1}) by multiplying the cell-specific uptake rates (fg N $cell^{-1}$ h^{-1}) by the average in situ abundance of each group (cells L^{-1}) observed in the SCM (Table 4). As the NFP were the most abundant group (5.39×10^8 cell L^{-1}) compared with *Prochlorococcus* (5.53×10^7 cell L^{-1}) and *Synechococcus*-like (1.05×10^7 cell L^{-1}), they dominated uptake rates for all forms of N measured (Table 4). The uptake rates of oxidized forms of N were 14.07 ng N L^{-1} d^{-1} for NO_3^- and 1.86 ng N L^{-1} d^{-1} for NO_2^-, 2–3 orders of magnitude higher

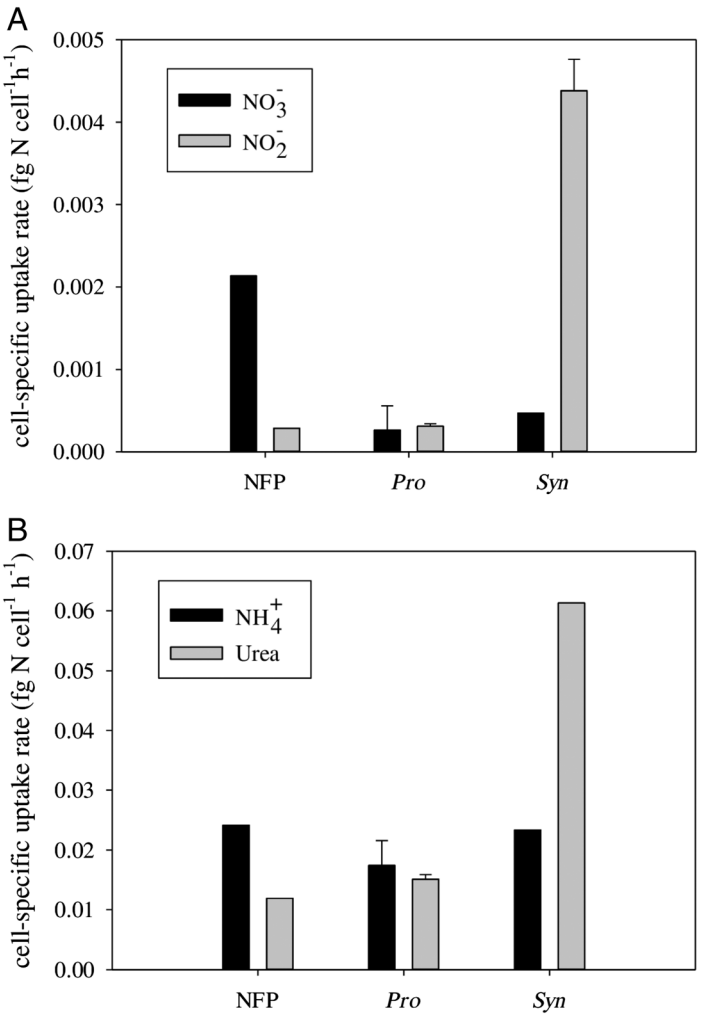

Fig. 4. Cell-specific uptake rates (fg N cell^{-1} h^{-1}) for NFP, *Prochlorococcus* (*Pro*), and *Synechococcus*-like (*Syn*) collected from the SCM: (**A**) NO_3^- and NO_2^- uptake and (**B**) NH_4^+ and urea uptake.

than the uptake rates measured for *Prochlorococcus* and *Synechococcus*-like groups. The potential uptake rates of reduced forms of N by NFP were 313.74 ng N L^{-1} d^{-1} for NH_4^+ and 154.84 ng N L^{-1} d^{-1} for urea, 1–2 orders of magnitude higher than those estimated for *Prochlorococcus* and *Synechococcus*-like. For *Prochlorococcus*, the potential uptake rates for NH_4^+ and urea were similar to each other, at 23.23 ng N L^{-1} d^{-1} and 20.16 ng N L^{-1} d^{-1}, respectively. *Synechococcus*-like had a potential uptake rates similar to *Prochlorococcus* for urea (15.53 ng N L^{-1} d^{-1}) but lower for NH_4^+ (5.91 ng N L^{-1} d^{-1}).

δ^{15}N vs. environmental variables

Pearson correlation analyses revealed a strong negative correlation between the δ^{15}N of *Prochlorococcus* and NO_3^- concentrations ($r = -0.82$; p value = 0.01) and positive correlation with NH_4^+ concentrations ($r = 0.72$; p value = 0.03) (Supporting Information Table S6). However, there were no significant correlations between δ^{15}N of *Prochlorococcus* and percent light or NO_2^- concentrations. There were no significant correlations between the δ^{15}N of *Synechococcus*-like inhabiting the SCM and any of the tested variables.

Discussion

Oceanographic conditions and SCM

Previous studies that analyzed SCMs found conditions within the range observed here (Lavin et al. 2010; Garcia-Robledo et al. 2017; Widner et al. 2018*a*,*b*). Dissolved oxygen shows saturation conditions at the surface layer, followed by a pronounced oxycline. Between 62 and 130 m depth (depending on the station) oxygen decreases to undetectable levels. Bellow this depth, a SCM develops in oxygen-depleted and NO_3^- rich conditions, but with low concentrations of reduced N as NH_4^+ or urea (Table 2; Fig. 2).

Table 4. Cell-specific (fg N cell^{-1} h^{-1}) and group-specific (ng N L^{-1} d^{-1}) uptake rates of oxidized (NO_3^- and NO_2^-) and reduced (NH_4^+ and urea) N forms measured in this study for each group of sorted cells: NFP, *Prochlorococcus* (*Pro*), and *Synechococcus*-like (*Syn*). Group-specific uptake rates were calculated multiplying the cell-specific uptake rates (fmol cell^{-1} d^{-1}) by the in situ average abundance of cells of each group (cell L^{-1}).

	Cell-specific uptake rates (fg N cell^{-1} h^{-1})				Group-specific uptake rates (ng N L^{-1} d^{-1})			
Group	NO_3^-	NO_2^-	NH_4^+*	**Urea***	NO_3^-	NO_2^-	NH_4^+*	**Urea***
NFP	**0.0022**	**0.0003**	**0.0243**	**0.0120**	**14.07**	**1.86**	**313.74**	**154.84**
Pro	**0.0003**	**0.0003**	**0.0175**	**0.0152**	**0.18**	**0.21**	**23.23**	**20.16**
	SD = 0.0003	SD = 0.00003	SD = 0.0042	SD = 0.0008	SD = 0.19	SD = 0.02	SD = 5.52	SD = 1.04
	n = 4	*n* = 2	*n* = 2	*n* = 2	*n* = 4	*n* = 2	*n* = 2	*n* = 2
Syn	**0.0005**	**0.0044**	**0.0235**	**0.0616**	**0.06**	**0.56**	**5.91**	**15.53**
		SD = 0.0004				SD = 0.05		
		n = 2				*n* = 2		

*Tracer additions resulted in initial enrichments > 50%, rates should be considered as potential uptake.

Prochlorococcus and *Synechococcus*-like numerically dominated the SCM picophytoplankton community and there were almost no detectable PPE. Apparently this pattern is a persistent characteristic of this particular environment as shown by the few previous studies in ODZs (Lavin et al. 2010; Astorga-Eló et al. 2015; Garcia-Robledo et al. 2017). The relative abundance of *Prochlorococcus* compared to the total picoplanktonic community was consistent with previously reported ranges (> 5.3%) (Lavin et al. 2010). Although the lineages of *Prochlorococcus* and *Synechococcus*-like composing the SCM community were not analyzed as part of this study, they have been previously identified using cloning and sequencing, and terminal restriction fragment length polymorphism analyses applied to the 16S–23S rRNA internal transcribed spacer region (Lavin et al. 2010). Lavin and colleagues found that > 90% of total *Prochlorococcus* in the SCM was composed by the lineage LLIV and two novel lineages termed LLV and LLVI. On other hand, *Synechococcus* was mainly represented by clade I and VI, but with very low abundances.

Assimilative N metabolism in ODZ picocyanobacteria

Natural abundance samples

The measurements of δ^{15}N-NO_3^- reported in the literature for the ODZs range from 12.4‰ to 17.2‰, and from −16.0‰ to −17.8‰ for δ^{15}N-NO_2^-, showing a difference up to 35‰ between both nitrogen sources (Casciotti and McIlvin 2007). These differences are considered a consequence of isotope fractionation during the processes of denitrification (Casciotti and McIlvin 2007) and nitrite oxidation (Peters et al. 2016). NH_4^+ and urea exhibit very low (nanomolar) concentrations in the ocean (for our study sites, see Table 2) and it has not been possible to measure their δ^{15}N to date, as the most sensitive methods require concentrations of at least 0.5 μmol L^{-1} (Zhang et al. 2007). However, NH_4^+ and urea would have an estimated value close to 7‰ (min = 1.3‰; max = 14.4‰; SD = 4.2‰) considering the average of 10‰ for PON_{sus} in the SCM (Supporting Information Table S7) or close to 5.1‰ if the NH_4^+ and urea come mainly by the degradation of sinking material as fecal pellets and/or marine snow (PON_{sk} ~ 8.1‰ in the ODZ; Fuchsman et al. 2018) (Table 3).

The δ^{15}N-PON_{sus} for the SCM samples was always positive, with values ranging from 4.3‰ to 16.6‰ (Fig. 3). The explanation for these relative high δ^{15}N could be the result of the assimilation of high δ^{15}N (as NO_3^-) by the community composing the SCM or the release of low δ^{15}N (as the case of anammox or denitrification) Thus, the δ^{15}N-PON_{sus} for the SCM represents a mixture of the δ^{15}N of diverse source pools, both living and nonliving. The relative contributions of the different components vary among stations, with δ^{15}N values that can be low for some components and high for others.

Another source of variability of δ^{15}N-PON_{sus} from SCMs at different stations may due to the potential variability in the composition of NFP. Although we identified a very abundant and consistent picophytoplankton component (*Prochlorococcus* and *Synechococcus*-like) in samples collected from the SCM, NFP including heterotrophic or chemoautotrophic bacteria and archaea were far more abundant and may vary greatly in functional composition in SCM samples from different stations (e.g., ETNP/ETSP or coastal/oceanic). Differences in the bacterial or archaeal composition may be reflected in differences in the nutritional preferences of the dominant bacterial or archaeal members and this may be reflected in their δ^{15}N. As the δ^{15}N-PON_{sus} in the SCM presented much higher values than their components (Fig. 3), part of the variability presented and heavy isotopic signature could also be due to the contribution of nonliving particulate material sinking from the surface with high δ^{15}N. That could be the case for stations sampled in the ETSP, where measurements of δ^{15}N-PON_{sus} for the SCM exceeding by 6.5‰, 10.0‰, 3.3‰, and 3.5‰ the values measured for the δ^{15}N-PON_{sus} in the PCM (Supporting Information Table S7, bold font). Thus, sinking particles can be experiencing degradation by both bacteria and zooplankton, which preferentially degrade low δ^{15}N-PON to NH_4^+, leaving the residual PON enriched in ^{15}N. Accordingly, these results emphasize the importance of the use of flow cytometry cell sorting to distinguish the living and nonliving components of the community and their contribution to the bulk δ^{15}N signature.

The δ^{15}N observed for sorted *Prochlorococcus* cells from the SCM ranged from −4.0‰ to 13.0‰ (range = 17‰), higher than the range previously observed for *Prochlorococcus* cells from the Sargasso Sea with values ranging from −4‰ to −1‰ (range = 3‰) (Fawcett et al. 2011). The smaller range in δ^{15}N values from the Sargasso Sea *Prochlorococcus* group may be due to a more stable nutrient environment relative to an ODZ SCM. *Prochlorococcus* from the Sargasso Sea preferentially assimilates recycled N sources such as NH_4^+ or amino acids (Fawcett et al. 2011). The highest δ^{15}N observed in ODZ *Prochlorococcus* was only seen once in a coastal station in the ETSP (cruise NBP1305, Sta. BB2) and may have been due to use of NO_3^- (Table 3) as the main N source. The lowest δ^{15}N value (−4.0‰) for *Prochlorococcus* was observed at a more oceanic station in the ETSP (cruise AT2626, Sta. 8). Since neither *Prochlorococcus* nor *Synechococcus* has the genes to fix N_2 (Latysheva et al. 2012), low δ^{15}N values could be evidence of NO_2^- assimilation, as NO_2^- is the only N source with negative δ^{15}N values. Fifty percent of the *Prochlorococcus* δ^{15}N values ranged from −2.1‰ to 2.6‰ (median of −0.6‰), suggesting that ODZ SCM *Prochlorococcus* is most likely assimilating a mixture of N sources with positive δ^{15}N as ammonium, urea, and/or NO_3^-, while assimilation of N sources with negative δ^{15}N such as NO_2^- may lower cellular δ^{15}N. Similar to *Prochlorococcus*, *Synechococcus*-like cells isolated from the ODZ SCM had δ^{15}N values ranging from −4.0‰ to 8.1‰ (range = 12.1) and had a broader range than values observed for Sargasso Sea *Synechococcus*, which ranged from −3‰ to −1‰ (range = 2) (Fawcett et al. 2011). Apparently both picocyanobacteria have similar nutritional preferences in the ODZ SCM.

No photosynthetic picoeukaryotes were observed in the ODZ SCM, while those found in the PCM presented $\delta^{15}N$ values ranging from −0.3‰ to 2.4‰, with 50% of the data (n = 5) ranging from 0.5‰ to 1.2‰. These values are one-order of magnitude lower than those reported for PPE in the Sargasso Sea at 100 m depth ($\delta^{15}N$ = 12.7‰), where PPE seems to be assimilating upwelled NO_3^- from below the euphotic zone, but close to those reported for lower depths ($\delta^{15}N$ between 1‰ and 5‰) where most phytoplankton growth is thought to be supported by NH_4^+ (Fawcett et al. 2011).

The question remains whether the high variability $\delta^{15}N$ of *Prochlorococcus* and *Synechococcus*-like might be explained by environmental factors such as light and/or nutrient concentration. It can be hypothesized that higher light availability might increase the probability that *Prochlorococcus* uses NO_3^- because it would have more energy available needed for NO_3^- assimilation. However, there was no significant correlation of $\delta^{15}N$ with light percentage, but instead a significant negative correlation with NO_3^- and positive correlations with NH_4^+ (Supporting Information Table S6). A negative correlation

Table 5. Comparison of cell-specific uptake rates (fg N cell^{-1} h^{-1}) by picophytoplankton in various regions of the ocean. ND indicates it was not detected.

	Cell-specific uptake rate (fg N cell^{-1} h^{-1})						
Microorganism	Urea	NH_4^+	NO_3^-	NO_2^-	Estimated total N rates*	Environment	Reference
Prochlorococcus	0.0152	0.0175	0.0003	0.0003	—	ODZ	This study
Synechococcus-like	0.0616	0.0235	0.0005	0.0044	—	ODZ	This study
NF picoplankton	0.0120	0.0243	0.0022	0.0003	—	ODZ	This study
Picophytoplankton	—	—	—	—	0.0711	SCM ODZ ETNP	Garcia-Robledo et al. (2017)
Picophytoplankton	—	—	—	—	0.0326	SCM ODZ ETNP	Garcia-Robledo et al. (2017)
Picophytoplankton	—	—	—	—	0.1304	SCM ODZ ETNP	Garcia-Robledo et al. (2017)
Picophytoplankton	—	—	—	—	ND	SCM ODZ ETNP	Garcia-Robledo et al. (2017)
Picophytoplankton	—	—	—	—	0.6521	SCM ODZ ETNP	Garcia-Robledo et al. (2017)
Picophytoplankton	—	—	—	—	0.2304	SCM ODZ ETNP	Garcia-Robledo et al. (2017)
Picophytoplankton	—	—	—	—	0.2642	SCM ODZ ETNP	Garcia-Robledo et al. (2017)
Picophytoplankton	—	—	—	—	0.3098	SCM ODZ ETNP	Garcia-Robledo et al. (2017)
Picophytoplankton	—	—	—	—	0.2260	SCM ODZ ETNP	Garcia-Robledo et al. (2017)
Picophytoplankton	—	—	—	—	0.6711	SCM ODZ ETNP	Garcia-Robledo et al. (2017)
Picophytoplankton	—	—	—	—	0.2785	SCM ODZ ETNP	Garcia-Robledo et al. (2017)
Picophytoplankton	—	—	—	—	0.2144	SCM ODZ ETNP	Garcia-Robledo et al. (2017)
Prochlorococcus	—	—	—	—	0.0150	ST. ALOHA, 75 m	Björkman et al. (2015)
Prochlorococcus	—	—	—	—	0.0650	ST. ALOHA, 75 m	Björkman et al. (2015)
Prochlorococcus	—	—	—	—	0.0038	North Atlantic, 60 m	Li (1994)
Prochlorococcus	—	—	—	—	0.0338	North Atlantic, 60 m	Li (1994)
Prochlorococcus	—	—	—	—	0.1013	North Atlantic, 1 m	Li (1994)
Prochlorococcus	—	—	—	—	0.1500	Northeast Atlantic, surface	Jardillier et al. (2010)
Prochlorococcus	—	—	—	—	0.0463	Atlantic Northern Gyre, 20 m	Hartmann et al. (2014)
Prochlorococcus	—	—	—	—	0.1063	Atlantic equatorial region, 20 m	Hartmann et al. (2014)
Prochlorococcus	—	—	—	—	0.0550	Atlantic Southern Gyre, 20 m	Hartmann et al. (2014)
Prochlorococcus	—	—	—	—	0.0625	Atlantic southern temperate waters, 20 m	Hartmann et al. (2014)
Synechococcus	—	—	—	—	0.0238	North Atlantic, 60 m	Li (1994)
Synechococcus	—	—	—	—	0.1025	North Atlantic, 60 m	Li (1994)
Synechococcus	—	—	—	—	0.9600	North Atlantic, 1 m	Li (1994)
Synechococcus	—	—	—	—	0.4250	Northeast Atlantic, surface	Jardillier et al. (2010)
Synechococcus	—	—	—	—	2.1375	Northeast Atlantic, surface	Jardillier et al. (2010)
Synechococcus	—	—	—	—	0.6188	Atlantic Northern Gyre, 20 m	Hartmann et al. (2014)
Synechococcus	—	—	—	—	0.8338	Atlantic equatorial region, 20 m	Hartmann et al. (2014)
Synechococcus	—	—	—	—	0.5675	Atlantic Southern Gyre, 20 m	Hartmann et al. (2014)
Synechococcus	—	—	—	—	0.2800	Atlantic Southern temperate waters, 20 m	Hartmann et al. (2014)

between $\delta^{15}N$ of *Prochlorococcus* with NO_3^- concentration might be explained by the isotope discrimination during the NO_3^- assimilation. In general, at the top of the ODZ, where the SCM is developed, the NO_3^- concentration is always high, although variable among stations. At lower NO_3^- concentrations, the NO_3^- remaining would be enriched in ^{15}N due to fractionation during assimilation, enriching the signal in *Prochlorococcus* that are still assimilating this NO_3^-. This possibility is supported by the results of $\delta^{15}N$ for *Prochlorococcus* in the coastal Sta. BB2 where the SCM is shallower (68–88 m depth) and the concentration of NO_3^- is lower compared with the oceanic stations where the SCMs are found at greater depths with higher concentration of NO_3^- (*see* Supporting Information Fig. S3). In the case of *Synechococcus*-like, $\delta^{15}N$ did not have any significant correlations with either the percentage of light or the concentrations of nutrients. In summary, our $\delta^{15}N$ natural abundance data from sorted groups of *Prochlorococcus* and *Synechococcus*-like suggest that these groups are using a mixture of different sources of N, mainly as NH_4^+ and urea, while in some instances NO_2^- or NO_3^- may be used preferentially to satisfy their N requirements.

Nitrogen assimilation rates

The cell-specific uptake rates of oxidized and reduced N forms for the different sorted groups (*Prochlorococcus*, *Synechococcus*-like and NFP) were compared with total N uptake rates reported for picophytoplankton in several study sites (Table 5). The results indicate that *Prochlorococcus* and *Synechococcus*-like are using NO_3^- and NO_2^- in the SCM at extremely low rates for their N requirements and that the potential rates for NH_4^+ and urea are comparable at least to some of the study sites listed in Table 5. It is also important to point out that this list in Table 5 shows high variability in the uptake rates (*see* Garcia-Robledo et al. 2017 for measurements for different stations in the SCM) and that our results are within this variability. The uptake rates obtained for the reduced N forms also support the data obtained for the natural abundance values of $\delta^{15}N$, where most of the natural abundance data for the picocyanobacteria were consistent with the $\delta^{15}N$ of NH_4^+/urea or a mixture of these sources including NO_3^- and NO_2^-. However, the results here are not yet sufficient to provide understanding of what controls the use of the different N sources.

Our results indicate that although ODZ *Prochlorococcus* have retained the capacity to use NO_3^- (Astorga-Eló et al. 2015; Widner et al. 2018*a*), they appear not to rely on NO_3^- as a principal N source. This suggests that ODZ *Prochlorococcus* are not under the high pressure for genome streamlining that other picocyanobacterial lineages experience. These findings are consistent with the basal characteristic of ODZ *Prochlorococcus* lineages linking this group with marine *Synechococcus* (Lavin et al. 2010), which has also not experienced significant genome streamlining (Dufresne et al. 2005; Partensky and Garczarek 2010). Thus, the ecological and evolutionary basis for the apparently strong niche preference of the ODZ *Prochlorococcus* for the low-light anoxic conditions of the SCM remains mysterious.

Implications for the ODZs

The fate of all nitrogen sources taken up by cyanobacteria is to be metabolized to NH_4^+, which is finally incorporated into the carbon backbones through glutamine synthetase-glutamate synthetase pathway, a key step to conversion from inorganic N forms to organic N forms such as amino acids or nucleic acids (García-Fernández and Diez 2004; Flores and Herrero 2005). Since all N sources other than NH_4^+ require intracellular conversion to NH_4^+, it is usually assumed that the most reduced forms of N (NH_4^+, urea, amino acids) will be the preferred N sources by cyanobacteria, as they require a lower energy expenditure for use. This is even more important in zones where the energy available is limited, as in the SCM (< 0.1% of the incident light) and where the oxidized N sources are abundant and the reduced ones are scarce. Then the selection of one or another N source is a balance between the energy needed to utilize that source and N availability in the environment.

ODZs present an active N cycle where processes like denitrification, anammox, and nitrification are known for the use and/or production of different forms of N (Lam and Kuypers 2011; Stewart et al. 2012). The low NH_4^+ concentrations have been explained by a coupling between the NH_4^+ produced during organic matter respiration by heterotrophic denitrification and a high anammox activity that converts NH_4^+ to N_2 (Richards et al. 1965; Devol 2003). However, it has recently been demonstrated that ODZ *Prochlorococcus* can contribute to aerobic metabolisms in the ODZs, such as nitrification and aerobic organic matter oxidation, through cryptic O_2 production in these zones (Garcia-Robledo et al. 2017). In that study, (meta)transcriptional analysis indicated a low anammox activity (possibly inhibited by *Prochlorococcus* O_2 production) and high NO_2^- and organic matter oxidation. These results can be interpreted as a possible NH_4^+ production due to organic matter oxidation, a decreased NH_4^+ consumption by the anammox bacteria and/or archaea (low transcripts), leaving available NH_4^+ for *Prochlorococcus* assimilation with no accumulation of NH_4^+ in the water column and explaining the high uptake rates of reduced N forms. However, NH_4^+ is still scarce, so NO_2^-, which is most abundant in the SCM, could represent the source of N needed for at least a percentage of the group of *Prochlorococcus* inhabiting the ODZ. Therefore, the uptake of NO_2^- by *Prochlorococcus* would mean an eventual competition for this nutrient with the highly active nitrite oxidizing bacteria in the SCM (Garcia-Robledo et al. 2017).

Conclusions

In summary, our results suggest that ODZ *Prochlorococcus* cyanobacteria are using a mixture of reduced and oxidized forms of N to satisfy their requirements. Nevertheless when NH_4^+ and urea are available, *Prochlorococcus* preferentially use

those nutrients even though their genetic repertoire permits the use of oxidized forms. The selection of reduced forms of N can be explained by the low energy needed to assimilate those N forms, important in the SCM (<0.1% of the incident light), but not for the availability of these nutrients in the SCM since they are scarce in ODZ. Perhaps the oxygen production by *Prochlorococcus* is stimulating aerobic respiration by heterotrophic bacteria and producing the NH_4^+ that *Prochlorococcus* needs with no accumulation in the SCM. Finally, our results suggest that ODZ picocyanobacteria might thus represent potential competitors with anammox bacteria or ammonia-oxidizing archaea for NH_4^+ and/or with nitrite oxidizing bacteria for NO_2^-.

References

Astorga-Eló, M., S. Ramírez-Flandes, E. F. DeLong, and O. Ulloa. 2015. Genomic potential for nitrogen assimilation in uncultivated members of *Prochlorococcus* from an anoxic marine zone. ISME J. **9**: 1264–1267. doi:10.1038/ismej.2015.21

Batmalle, C. S., H.-I. Chiang, K. Zhang, M. W. Lomas, and A. C. Martiny. 2014. Development and bias assessment of a method for targeted metagenomic sequencing of marine cyanobacteria. Appl. Environ. Microbiol. **80**: 1116–1125. doi:10.1128/AEM.02834-13

Berges, J. A., and M. R. Mulholland. 2008. Enzymes and nitrogen cycling, p. 1385–1444. *In* D. G. Capone, D. A. Bronk, M. R. Mulholland, and E. J. Carpenter [eds.], Nitrogen in the marine environment. Academic Press. doi:10.1016/B978-0-12-372522-6.00032-3

Berube, P. M., and others. 2015. Physiology and evolution of nitrate acquisition in *Prochlorococcus*. ISME J. **9**: 1195–1207. doi:10.1038/ismej.2014.211

Biller, S. J., P. M. Berube, D. Lindell, and S. W. Chisholm. 2014. *Prochlorococcus*: The structure and function of collective diversity. Nat. Rev. Microbiol. **13**: 13–27. doi:10.1038/nrmicro3378

Björkman, K. M., M. J. Church, J. K. Doggett, and D. M. Karl. 2015. Differential assimilation of inorganic carbon and leucine by *Prochlorococcus* in the oligotrophic North Pacific Subtropical Gyre. Front. Microbiol. **6**: 1–14. doi:10.3389/fmicb.2015.01401

Casciotti, K. L., and M. R. McIlvin. 2007. Isotopic analyses of nitrate and nitrite from reference mixtures and application to Eastern Tropical North Pacific waters. Mar. Chem. **107**: 184–201. doi:10.1016/j.marchem.2007.06.021

Casey, J. R., M. W. Lomas, J. Mandecki, and D. E. Walker. 2007. *Prochlorococcus* contributes to new production in the Sargasso Sea deep chlorophyll maximum. Geophys. Res. Lett. **34**: 1–5. doi:10.1029/2006GL028725

Chisholm, S. W. 1992. Phytoplankton size, p. 213–237. *In* P. G. Falkowski, A. D. Woodhead, and K. Vivirito [eds.], Primary productivity and biogeochemical cycles in the sea. Environmental science research, v. **43**. Springer. doi:10.1007/978-1-4899-0762-2_12

Devol, A. H. 2003. Nitrogen cycle: Solution to a marine mystery. Nature **422**: 575–576. doi:10.1038/422575a

Dufresne, A., L. Garczarek, and F. Partensky. 2005. Accelerated evolution associated with genome reduction in a free-living prokaryote. Genome Biol. **6**: R14. doi:10.1186/gb-2005-6-2-r14

Dugdale, R. C., and F. P. Wilkerson. 1986. The use of ^{15}N to measure nitrogen uptake in eutrophic oceans; experimental considerations. Limnol. Oceanogr. **31**: 673–689. doi:10.4319/lo.1986.31.4.0673

Fawcett, S. E., M. W. Lomas, J. R. Casey, B. B. Ward, and D. M. Sigman. 2011. Assimilation of upwelled nitrate by small eukaryotes in the Sargasso Sea. Nat. Geosci. **4**: 717–722. doi:10.1038/ngeo1265

Flombaum, P., and others. 2013. Present and future global distributions of the marine cyanobacteria *Prochlorococcus* and *Synechococcus*. Proc. Natl. Acad. Sci. USA **110**: 9824–9829. doi:10.1073/pnas.1307701110

Flores, E., and A. Herrero. 2005. Nitrogen assimilation and nitrogen control in cyanobacteria. Biochem. Soc. Trans. **33**: 164–167. doi:10.1042/BST0330164

Fuchsman, C. A., A. H. Devol, K. L. Casciotti, C. Buchwald, B. X. Chang, and R. E. A. Horak. 2018. An N isotopic mass balance of the Eastern Tropical North Pacific oxygen deficient zone. Deep-Sea Res. Part II Top. Stud. Oceanogr. **156**: 137–147. doi:10.1016/j.dsr2.2017.12.013

Fuhrman, J. 2003. Genome sequences from the sea. Nature **424**: 1001–1002. doi:10.1038/4241001a

García-Fernández, J. M., N. T. de Marsac, and J. Diez. 2004. Streamlined regulation and gene loss as adaptive mechanisms in *Prochlorococcus* for optimized nitrogen utilization in oligotrophic environments. Microbiol. Mol. Biol. Rev. **68**: 630–638. doi:10.1128/MMBR.68.4.630-638.2004

García-Fernández, J. M., and J. Diez. 2004. Adaptive mechanisms of nitrogen and carbon assimilatory pathways in the marine cyanobacteria *Prochlorococcus*. Res. Microbiol. **155**: 795–802. doi:10.1016/j.resmic.2004.06.009

Garcia-Robledo, E., C. C. Padilla, M. Aldunate, F. J. Stewart, O. Ulloa, A. Paulmier, G. Gregori, and N. P. Revsbech. 2017. Cryptic oxygen cycling in anoxic marine zones. Proc. Natl. Acad. Sci. USA **114**: 8319–8324. doi:10.1073/pnas.1619844114

Garside, C. 1982. A chemiluminescent technique for the determination of nanomolar concentrations of nitrate and nitrite in seawater. Mar. Chem. **11**: 159–167. doi:10.1016/0304-4203(82)90039-1

Goericke, R., R. Olson, and A. Shalapyonok. 2000. A novel niche for *Prochlorococcus* sp. in low-light suboxic environments in the Arabian Sea and the Eastern Tropical North Pacific. Deep-Sea Res. Part I Oceanogr. Res. Pap. **47**: 1183–1205. doi:10.1016/S0967-0637(99)00108-9

Granger, J., D. M. Sigman, M. M. Rohde, M. T. Maldonado, and P. D. Tortell. 2010. N and O isotope effects during nitrate assimilation by unicellular prokaryotic and eukaryotic

plankton cultures. Geochim. Cosmochim. Acta **74**: 1030–1040. doi:10.1016/j.gca.2009.10.044

Hamersley, M. R., and others. 2007. Anaerobic ammonium oxidation in the Peruvian oxygen minimum zone. Limnol. Oceanogr. **52**: 923–933. doi:10.4319/lo.2007.52.3.0923

Hartmann, M., P. Gomez-Pereira, C. Grob, M. Ostrowski, D. J. Scanlan, and M. V. Zubkov. 2014. Efficient CO_2 fixation by surface *Prochlorococcus* in the Atlantic Ocean. ISME J. **8**: 2280–2289. doi:10.1038/ismej.2014.56

Holmes, R. M., A. Aminot, R. Kerouel, B. A. Hooker, and B. J. Peterson. 1999. A simple and precise method for measuring ammonium in marine and freshwater ecosystems. Can. J. Fish. Aquat. Sci. **56**: 1801–1808. doi:10.1139/f99-128

Jardillier, L., M. V. Zubkov, J. Pearman, and D. J. Scanlan. 2010. Significant CO_2 fixation by small prymnesiophytes in the subtropical and tropical northeast Atlantic Ocean. ISME J. **4**: 1180–1192. doi:10.1038/ismej.2010.36

Johnson, Z. I., E. R. Zinser, A. Coe, N. P. McNulty, E. M. S. Woodward, and S. W. Chisholm. 2006. Niche partitioning among *Prochlorococcus* ecotypes along ocean-scale environmental gradients. Science **311**: 1737–1740. doi:10.1126/science.1118052

Kamennaya, N. A., and A. F. Post. 2011. Characterization of cyanate metabolism in marine *Synechococcus* and *Prochlorococcus* spp. Appl. Environ. Microbiol. **77**: 291–301. doi:10.1128/AEM.01272-10

Lam, P., and M. M. M. Kuypers. 2011. Microbial nitrogen cycling processes in oxygen minimum zones. Ann. Rev. Mar. Sci. **3**: 317–345. doi:10.1146/annurev-marine-120709-142814

Latysheva, N., V. L. Junker, W. J. Palmer, G. A. Codd, and D. Barker. 2012. The evolution of nitrogen fixation in cyanobacteria. Bioinformatics **28**: 603–606. doi:10.1093/bioinformatics/bts008

Lavin, P., B. González, J. F. Santibáñez, D. J. Scanlan, and O. Ulloa. 2010. Novel lineages of *Prochlorococcus* thrive within the oxygen minimum zone of the eastern tropical South Pacific. Environ. Microbiol. Rep. **2**: 728–738. doi:10.1111/j.1758-2229.2010.00167.x

Li, W. K. W. 1994. Primary production of prochlorophytes, cyanobacteria, and eucaryotic ultraphytoplankton: Measurements from flow cytometric sorting. Limnol. Oceanogr. **39**: 169–175. doi:10.4319/lo.1994.39.1.0169

Marie, D., F. Partensky, D. Vaulot, and C. Brussaard. 1999. Enumeration of Phytoplankton, Bacteria, and Viruses in Marine Samples, p. 11.11.1–11.11.15. In J.P.E.A Robinson [ed.], Current protocols in cytometry, suppl. 10. John Wiley & Sons Inc., New York. N.Y. doi:10.1002/0471142956.cy1111s10

Martiny, A. C., A. P. K. Tai, D. Veneziano, F. Primeau, and S. W. Chisholm. 2009. Taxonomic resolution, ecotypes and the biogeography of *Prochlorococcus*. Environ. Microbiol. **11**: 823–832. doi:10.1111/j.1462-2920.2008.01803.x

McIlvin, M. R., and K. L. Casciotti. 2011. Technical updates to the bacterial method for nitrate isotopic analyses. Anal. Chem. **83**: 1850–1856. doi:10.1021/ac1028984

Moore, L. R., G. Rocap, and S. W. Chisholm. 1998. Physiology and molecular phylogeny of coexisting *Prochlorococcus* ecotypes. Nature **393**: 464–467. doi:10.1038/30965

Moore, L. R., and S. W. Chisholm. 1999. Photophysiology of the marine cyanobacterium *Prochlorococcus*: Ecotypic differences among cultured isolates. Limnol. Oceanogr. **44**: 628–638. doi:10.4319/lo.1999.44.3.0628

Moore, L. R., A. F. Post, G. Rocap, and S. W. Chisholm. 2002. Utilization of different nitrogen sources by the marine cyanobacteria *Prochlorococcus* and *Synechococcus*. Limnol. Oceanogr. **47**: 989–996. doi:10.4319/lo.2002.47.4.0989

Owens, N. J. P. 1987. Natural variations in ^{15}N in the marine environment, p. 389–451. In J. H. S. Blaxter and A. J. Southward [eds.], Advances in Marine Biology. Academic Press Inc. London, Great Britain.

Partensky, F., J. Blanchot, and D. Vaulot. 1999*a*. Differential distribution and ecology of *Prochlorococcus* and *Synechococcus* in oceanic waters: A review. Bull. l'Institut océanographique **19**: 457–475.

Partensky, F., W. R. Hess, and D. Vaulot. 1999*b*. *Prochlorococcus*, a marine photosynthetic prokaryote of global significance. Microbiol. Mol. Biol. Rev. **63**: 106–127.

Partensky, F., and L. Garczarek. 2010. *Prochlorococcus*: Advantages and limits of minimalism. Ann. Rev. Mar. Sci. **2**: 305–331. doi:10.1146/annurev-marine-120308-081034

Peters, B., R. Horak, A. Devol, C. Fuchsman, M. Forbes, C. W. Mordy, and K. L. Casciotti. 2018. Estimating fixed nitrogen loss and associated isotope effects using concentration and isotope measurements of NO_3^-, NO_2^-, and N_2 from the Eastern Tropical South Pacific oxygen deficient zone. Deep-Sea Res. Part II Top. Stud. Oceanogr. **156**: 121–136. doi:10.1016/j.dsr2.2018.02.011

Peters, B. D., A. R. Babbin, K. A. Lettmann, C. W. Mordy, O. Ulloa, B. B. Ward, and K. L. Casciotti. 2016. Vertical modeling of the nitrogen cycle in the eastern tropical South Pacific oxygen deficient zone using high-resolution concentration and isotope measurements. Global Biogeochem. Cycles **30**: 1661–1681. doi:10.1002/2016GB005415

Revsbech, N. P., L. H. Larsen, J. Gundersen, T. Dalsgaard, O. Ulloa, and B. Thamdrup. 2009. Determination of ultra-low oxygen concentrations in oxygen minimum zones by the STOX sensor. Limnol. Oceanogr.: Methods **7**: 371–381. doi:10.4319/lom.2009.7.371

Richards, F. A., J. D. Cline, W. W. Bronkow, and L. P. Atkinson. 1965. Some consequences of the decomposition of organic matter in Lake Nitinat, an anoxic fjord. Limnol. Oceanogr. **10**: 185–201. doi:104319/lo.1965.10.suppl2.r185

Rocap, G., and others. 2003. Genome divergence in two *Prochlorococcus* ecotypes reflects oceanic niche differentiation. Nature **424**: 1042–1047. doi:10.1038/nature01947

Santoro, A. E., and others. 2013. Measurements of nitrite production in and around the primary nitrite maximum in the Central California Current. Biogeosciences **10**: 7395–7410. doi:10.5194/bg-10-7395-2013

Scanlan, D. J. 2003. Physiological diversity and niche adaptation in marine *Synechococcus*. Adv. Microb. Physiol. **47**: 1–64. doi:10.1016/S0065-2911(03)47001-X

Sigman, D. M., and K. L. Casciotti. 2001. Nitrogen isotopes in the ocean, p. 1884–1894. In J. H. Steele, K. K. Turekian, and S. A. Thorpe [eds.], Encyclopedia of Ocean Sciences. Academic Press Inc. London, Great Britain.

Sigman, D. M., K. L. Casciotti, M. Andreani, C. Barford, M. Galanter, and J. K. Böhlke. 2001. A bacterial method for the nitrogen isotopic analysis of nitrate in seawater and freshwater. Anal. Chem. **73**: 4145–4153. doi:10.1021/ac010088e

Stewart, F. J., O. Ulloa, and E. F. Delong. 2012. Microbial metatranscriptomics in a permanent marine oxygen minimum zone. Environ. Microbiol. **14**: 23–40. doi:10.1111/j.1462-2920.2010.02400.x

Thamdrup, B., T. Dalsgaard, M. M. Jensen, O. Ulloa, L. Farías, and R. Escribano. 2006. Anaerobic ammonium oxidation in the oxygen-deficient waters off northern Chile. Limnol. Oceanogr. **51**: 2145–2156. doi:10.4319/lo.2006.51.5.2145

Thamdrup, B., T. Dalsgaard, and N. P. Revsbech. 2012. Widespread functional anoxia in the oxygen minimum zone of the Eastern South Pacific. Deep-Sea Res. Part I Oceanogr. Res. Pap. **65**: 36–45. doi:10.1016/j.dsr.2012.03.001

Ulloa, O., D. E. Canfield, E. F. DeLong, R. M. Letelier, and F. J. Stewart. 2012. Microbial oceanography of anoxic oxygen minimum zones. Proc. Natl. Acad. Sci. USA **109**: 15996–16003. doi:10.1073/pnas.1205009109

Ward, B. B., A. H. Devol, J. J. Rich, B. X. Chang, S. E. Bulow, H. Naik, A. Pratihary, and A. Jayakumar. 2009. Denitrification as the dominant nitrogen loss process in the Arabian Sea. Nature **461**: 78–81. doi:10.1038/nature08276

Waser, N. A. D., P. J. Harrison, B. Nielsen, S. E. Calvert, and D. H. Turpin. 1998. Nitrogen isotope fractionation during the uptake and assimilation of nitrate, nitrite, ammonium, and urea by a marine diatom. Limnol. Oceanogr. **43**: 215–224. doi:10.4319/lo.1998.43.2.0215

West, N. J., W. A. Schönhuber, N. J. Fuller, R. I. Amann, R. Rippka, A. F. Post, and D. J. Scanlan. 2001. Closely related *Prochlorococcus* genotypes show remarkably different depth distributions in two oceanic regions as revealed by in situ hybridization using 16S rRNA-targeted oligonucleotides. Microbiology **147**: 1731–1744. doi:10.1099/00221287-147-7-1731

Widner, B., C. A. Fuchsman, B. X. Chang, G. Rocap, and M. R. Mulholland. 2018*a*. Utilization of urea and cyanate in waters overlying and within the eastern tropical north Pacific oxygen deficient zone. FEMS Microbiol. Ecol. **94**: 1–15. doi:10.1093/femsec/fiy138

Widner, B., C. W. Mordy, and M. R. Mulholland. 2018*b*. Cyanate distribution and uptake above and within the Eastern Tropical South Pacific oxygen deficient zone. Limnol. Oceanogr. **63**: S177–S192. doi:10.1002/lno.10730

Zhang, L., M. A. Altabet, T. Wu, and O. Hadas. 2007. Sensitive measurement of NH_4^+ $^{15}N/^{14}N$ ($\delta^{15}NH_4^+$) at natural abundance levels in fresh and saltwaters. Anal. Chem. **79**: 5297–5303. doi:10.1021/ac070106d

Zubkov, M. V., B. M. Fuchs, G. A. Tarran, P. H. Burkill, and R. Amann. 2003. High rate of uptake of organic nitrogen compounds by *Prochlorococcus* cyanobacteria as a key to their dominance in oligotrophic oceanic waters. Microbiology **69**: 1299–1304. doi:10.1128/AEM.69.2.1299

Acknowledgments

We would like to thank chief scientists Alan Devol (NPB1305), Frank Stewart (NH1410), and Amal Jayakumar (RB1603). We would also like to thank the captains, crews, and scientific support personnel of the R/V *Nathaniel B. Palmer*, the R/V *New Horizon*, the R/V *Atlantis*, and the R/V *Ronald Brown*. We also thank Gadiel Alarcón, Marguerite Blum, and Francisco Chavez for help with the PPS; Cristian Venegas for assistance with flow cytometry analysis; and Brian Peters and Karen Casciotti for $\delta^{15}NO_3^-$ isotope data from cruise AT2626. This study was financially supported by the Millennium Science Initiative (grant IC 120019), the Chilean National Commission for Scientific and Technological Research (grant Fondecyt 1161483 to O.U.; grants Conicyt-USA 20120014 and FONDEQUIP EQM130267 to P.v.D.; and a graduate fellowship to M.A.) the National Science Foundation (grant OCE-1356056 to MRM). Additional support has been provided by REDOC project of Universidad de Concepción.

Conflict of Interest

None declared.

Submitted 11 January 2019
Revised 21 June 2019
Accepted 10 August 2019

Associate editor: James Moffett